Modeling Surface Runoff

– A Case Study of a Cultivated Field in Southern Finland

Harri Koivusalo and Tuomo Karvonen
Helsinki University of Technology, Espoo, Finland

The objective of this study was to compare approaches to modeling surface runoff due to summer and autumn storms on a cultivated field. The data consisted of measurements performed every 15 minutes during rainfall-surface runoff events in 1993. A transfer function model was formulated using measured rainfall or rainfall excess as an input and surface runoff as an output. The physical models were based on the kinematic wave approximation of the Saint Venant equations. Surface runoff was assumed to flow first as an overland flow on a level field and second in rills. The results showed that the transfer function model using rainfall excess as an input, and the implicitly solved rill flow model performed the best with respect to the fitness coefficients, which denoted the efficiency of the model. The testing of the models using fixed parameter combinations indicated that an event based parameter estimation was not applicable in verifying the models to changing conditions.

Introduction

Many of the runoff measurements taken in Finland have been carried out on small catchments. The main interest of the studies has been to evaluate the seasonal role of non-point source pollution in lakes and rivers. Modeling of surface runoff has involved the use of empirical approaches or prepared hydrological submodels of the non-point source pollution models (Mustonen 1963; Kauppi 1982; Seuna 1983; Rekolainen and Posch 1993). The comparison of different surface runoff models under

Finnish conditions has had few applications. In this study, modeling approaches in predicting individual surface runoff events were tested. The rainfall-runoff data were measured at the experimental field, which was normally cultivated. The 15-minute measuring frequency was selected to catch individual short-duration surface runoff peaks. The main purpose of the experimental field was to examine the effects of controlled drainage (Evans *et al.* 1989) on crop yield and sediment and nutrient loads. In addition, elementary research was carried out on soil water movement, snowmelt, drainage, and surface runoff (Laikari and Karvonen 1992).

The selected modeling approaches involved empirical and physical models. The empirical models were simple transfer functions describing a linear relationship between rainfall and surface runoff (*e.g.* Young 1984). In addition, the idea of rainfall excess as the surface runoff-generating component and its linear transformation to runoff were studied. More profound examples of the subject are found in Novotny and Shuhai (1989) and Jakeman *et al.* (1990). The physical models were based on the kinematic wave equations, which have numerous applications in the literature (Wooding 1965; Li *et al.* 1975; Parlange *et al.* 1981; Pearson 1989). In the physical models, surface runoff was assumed to flow first as sheet flow and second in rills.

Site Description and Data

The rainfall-runoff events were measured in summer and autumn 1993 at the experimental field of the Laboratory of Water Resources Engineering, Helsinki University of Technology. The field is located at Kirkkonummi in southern Finland, about 40 km west of Helsinki (Fig. 1). At the field, surface runoff measurements focused on two sections of spring wheat cultivated during summer 1993; the soil was silt and clay.

Surface runoff from the two sections was measured separately by collecting the runoff at the lowest points of the sections, where a measurement weir was built. The downslope sides of the sections were embanked to prevent runoff losses. The flow in the weir was obtained by measuring the water level in front of the weir with an ultrasound sensor. Rainfall was measured in two locations on the field as 15-minute accumulations using rain gauges of vertical tubes with a cone top and a hydrostatic pressure sensor.

The measurement system was real-time operating and was set up using data loggers installed on the field. The sensors were switched to the loggers which performed the measurements every 15 minutes by programmed commands. Radio modems, connected to the loggers, transferred the results to the main computer located in a building near the field. The computer stored the data on a hard disk and was connected to the telephone network through a modem, enabling a real-time connection from the laboratory to the field.

Most of the rainfall-runoff events on the two sections were measured during sum-
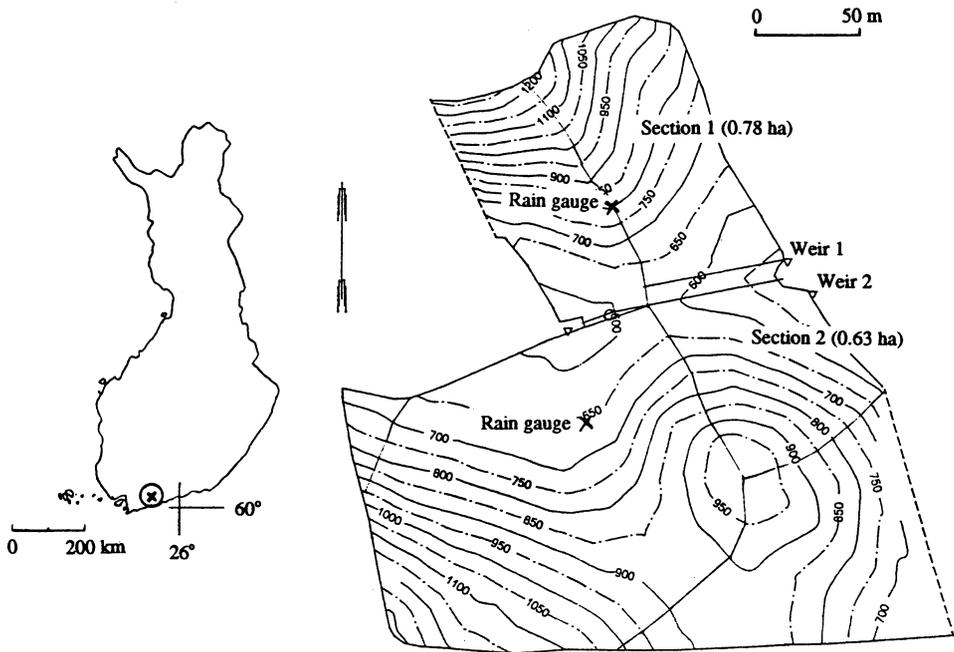
206

Fig. 1. Location of Sjökulla experimental field, surface runoff sections, and rain gauges.

mer and autumn 1993. In late June and early July, the measurement system had breaks lasting several days and the events in that time were not measured. In addition, the system was down during the morning when data were transferred from the main computer to the laboratory. In all, 86% of the 15-minute rainfall and surface runoff data were available during the measurement period June 1-October 18.

During data processing, missing 15-minute surface runoff values were set to zero. Measurement errors in precipitation resulted in apparent small values during rainless time periods. Therefore, precipitation values less than the measurement accuracy (0.13 mm/15 min) were not taken into account. During the runoff measurements, the voltage deviation did not greatly influence the zero values, because during periods without runoff the water level fell distinctly below the v-notch of the weirs.

Early summer 1993 was dry in June; the first heavy rains did not generate much surface runoff because the soil was heavily cracked with a large infiltration capacity. In August, the groundwater level rose frequently to the topsoil, which became saturated; small rainfalls also began to cause surface runoff. In late August, the groundwater level remained high, resulting in the highest summer runoff peaks. September was cold with several night-time temperatures $< 0°C$, inducing errors in the precipitation measurements. In October, the autumn storms began, causing a rapid rise in the groundwater level and much surface runoff.
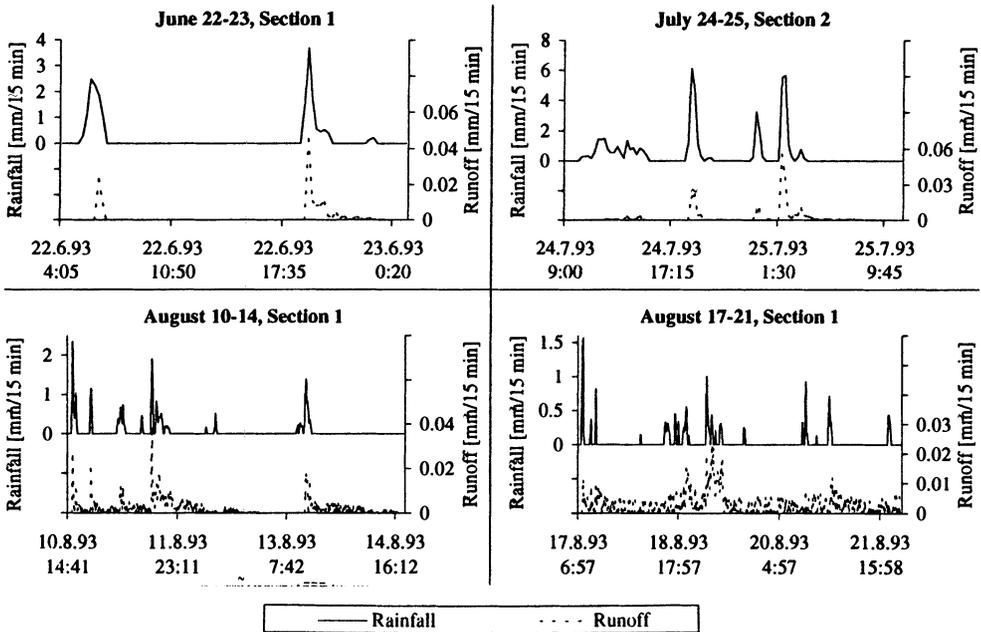
207

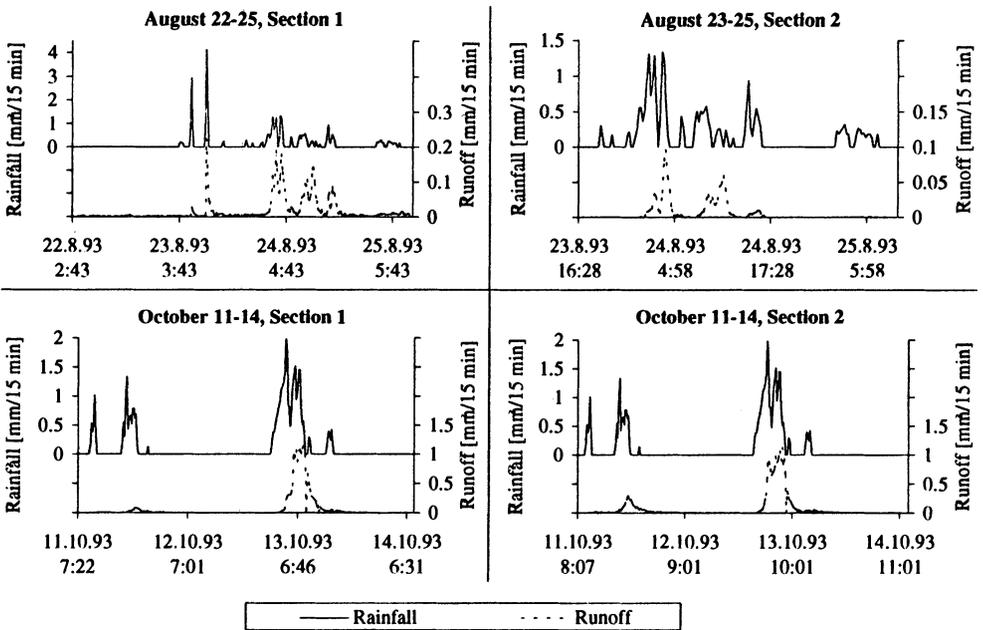Fig. 2. Surface runoff events measured during summer 1993.

Fig. 3. Surface runoff events measured during late summer-autumn 1993.

208

Table 1 – Times and some characteristics of measured rainfall-runoff events

Time	Total rainfall (mm)	Total runoff (mm)	Max rainfall (mm/15 mm)	Max runoff (mm/15 mm)
22.6.1993 4:05-23.6.1993 1:05	18	0.13	3.7	0.046
24.7.1993 9:00-25.7.1993 11:00	48	0.22	6.1	0.056
10.8.1993 14:41-14.8.1993 18:57	31	0.79	2.3	0.038
17.8.1993 6:57-21.8.1993 23:13	22	1.3	1.6	0.022
22.8.1993 2:43-25.8.1993 10:13	39	5.0	4.1	0.22
23.8.1993 16:28-25.8.1993 9:43	26	0.93	1.3	0.096
11.10.1993 7:22-14.10.1993 7:46	41	19	2.0	1.1
11.10.1993 8:07-14.10.1993 12:46	41	23	2.0	1.1

The field was seeded with spring wheat on May 3; by early June the soil was covered by the crop. The wheat was harvested on September 1 and the soil ploughed on October 4. In a part of Section 1, the controlled drainage was on all summer until August 18, when it was turned off; on October 7, it was turned on again.

After the data examination, eight surface runoff events were selected for the model testing. The events were required to cover evenly the time period under study. During early summer, smaller events were selected, while during late summer only the most inclusive events were selected. The smallest runoff events were not taken into account because their hydrographic shapes were often in conflict with the shapes of the rainfalls, which was due to the sum of errors in the measurements. Selected surface runoff events in Sections 1 and 2 are presented in Figs. 2-3 and some of their characteristics listed in Table 1.

Methods

Transfer Function Models

A linear relationship between measured rainfall and surface runoff was described by a simple transfer function model

$$\hat{q}_t = a_1 \hat{q}_{t-1} + a_2 \hat{q}_{t-2} + a_3 \hat{q}_{t-3} + b_1 p_t + b_2 p_{t-1} + b_3 p_{t-2} \tag{1}$$

where

$\hat{q}_t$ — surface runoff at time instant t (mm/15 min)
p_t — measured rainfall at time instant t (mm/15 min)
a_i, b_i — parameters
$t-1$ — previous (15 min) time instant

The 15-minute runoff prediction was based on the three previous predicted runoff values and the three rainfall values, of which the time of the first one corresponded
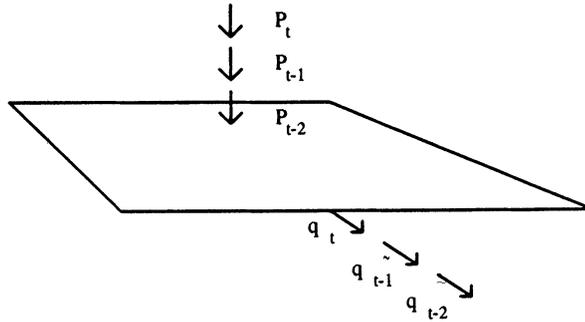
209

Fig. 4. Description of transfer function model between measured rainfall and surface runoff. Symbols are defined in Eq. (1).
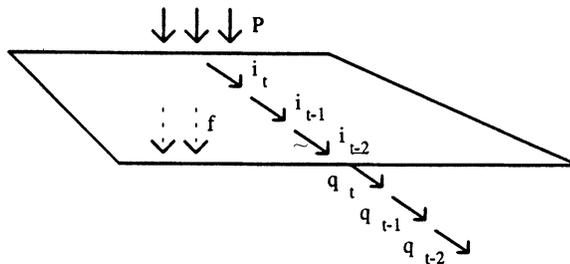
Fig. 5. Description of transfer function model between rainfall excess and surface runoff. Symbols are defined in Eqs. (1)-(4).

to the runoff prediction time (Fig. 4). This was according to the highest cross-correlation between rainfall and runoff calculated with zero delay during summer runoff events.

In the next stage, the transfer function model was formulated using rainfall excess instead of overall rainfall. Rainfall excess was calculated by subtracting infiltrated water from the measured rainfall (Fig. 5). The infiltration capacity was evaluated using a modified Green-Ampt infiltration equation (Skaggs 1980)

$$f = \frac{K_A}{F} + K_B \qquad (2)$$

where

f − infiltration capacity (mm/15 min)
F − cumulative infiltration (mm)
K_A, K_B − infiltration parameters

According to the equation, the infiltration capacity decreased as the cumulative infiltration increased. Parameter K_A implied the speed of the decrease, and parameter

210

K_B the hydraulic conductivity of the wet soil. The infiltration parameter values were estimated in the model calibration. After a dry period, the cumulative infiltration was set to a small value, raising the infiltration capacity to the initial value. The infiltration model was chosen to describe the behaviour of the cracked soil. The cracks affected the hydraulic conductivity of the saturated soil; therefore, a simple infiltration model, *e.g.* Eq. (2), was selected. The transfer function model between rainfall excess and surface runoff became

$$\hat{q}_t = a_1 \hat{q}_{t-1} + a_2 \hat{q}_{t-2} + a_3 \hat{q}_{t-3} + b_1 i_t + b_2 i_{t-1} + b_3 i_{t-2} \tag{3}$$

$$i_t = P_t - f_t \, , \qquad P_t > f_t \tag{4a}$$

$$i_t \equiv 0 \, , \qquad P_t \le f_t \tag{4b}$$

where

i_t – rainfall excess (mm/15 min)

Physical Runoff Models

Physical runoff models were based on the kinematic wave approximation of the Saint Venant equations. The continuity equation and a simplified version of the momentum equation can be written as

$$\frac{\partial h}{\partial t} + \frac{\partial q}{\partial x} = i \tag{5}$$

$$S_f = S \tag{6}$$

where

q – runoff per unit width (m³/s/m)
h – overland flow depth (m)
i – rainfall excess (m/s)
x – position from the top of the hillslope (m)
S_f – friction slope (m/m)
S – hill slope (m/m)

The rainfall excess was calculated based on Eqs. (2) and (4). Runoff per unit width was defined using the Manning equation for water velocity

$$v = \frac{1}{n} R_h^{2/3} S^{1/2} \tag{7}$$

where

v – water velocity (m/s)
R_h – hydraulic radius (m)
n – roughness coefficient

A value for roughness coefficient was estimated in the model calibration. Two ap-

211
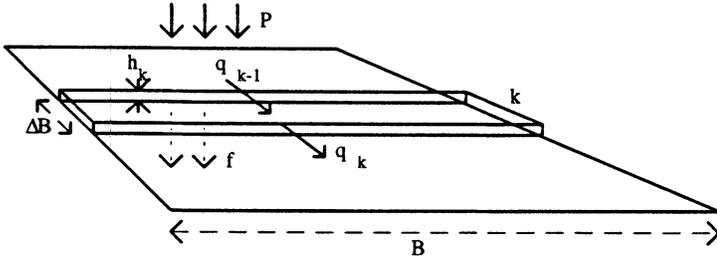
Fig. 6. Description of physical model for sheet flow. Symbols are defined in Eqs. (5)-(9).
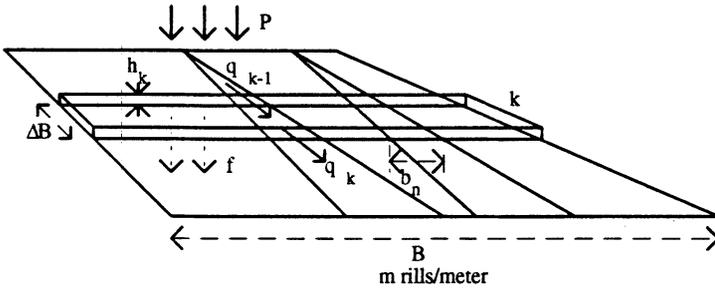
Fig. 7. Description of physical model for rill flow. Symbols are defined in Eqs. (5)-(11).

proaches were considered in calculating the runoff per unit width. At first, surface runoff was assumed to flow as a thin layer on the field (sheet flow, Fig. 6). Since the overland flow depth was small compared with the width of the field, the hydraulic radius was approximated

$$R_h = \frac{Bh}{B+2h} \approx h \tag{8}$$

where

R_h – hydraulic radius (m)
B – width of the field section (m)

Subsequently, in the case of the sheet flow model, runoff per unit width followed

$$q = \frac{1}{n} h^{5/3} S^{1/2} \tag{9}$$

Second, the runoff per unit width was assumed to flow in rills, and their dimensions were assumed to be known (rill flow, Fig. 7). The hydraulic radius was calculated as

$$R_h = \frac{b_n h}{b_n + 2h} \tag{10}$$

where

212

b_n – width of a rill (m)

The rills per unit width was taken as a parameter, and, in the case of the rill flow model, the runoff per unit width was

$$q = \frac{1}{n} \left(\frac{b_n h}{b_n + 2h} \right)^{2/3} S^{1/2} b_n hm \qquad (11)$$

where

m – number of rills per meter (1/m)

The sheet and rill flow models were solved using the Euler and Newton-Rhapson methods (*e.g.*, Conte and de Boor 1981). In each of the methods, the shape of the field section was assumed to be a square subdivided into N equal-sized rectangular node areas lying across the slope. The movement of water between the node areas at a certain time was evaluated forming an ordinary differential equation

$$\frac{dh_k}{dt} \equiv i - \frac{q_k - q_{k-1}}{\Delta B} \equiv F_k \qquad (12)$$

$$\mathbf{F} \equiv (F_k), \qquad k = 1, \ldots, N \qquad (13)$$

where

ΔB – length of the node area (m)
k – node area index
N – number of node areas

The runoff per unit width was constrained for inflow $q_0 \equiv 0$ in the top node.

The Euler method gave an explicit solution to the models, determining the flow depth based on the depth of the previous time instant, and in vector form was

$$\mathbf{h}_t = \mathbf{h}_{t-1} + \Delta t \mathbf{F}(\mathbf{h}_{t-1}) \qquad (14)$$

$$\mathbf{h}_t \equiv (h_{k,t}), \qquad k = 1, \ldots, N \qquad (15)$$

where

Δt – time step

$\mathbf{F}$ equaled Eq. (13). The Newton-Rhapson method gave an iterative solution to the flow depth $\mathbf{h}_t$ in the equation

$$h_{k,t} - h_{k,t-1} - \Delta t F_k = G_k = 0 \qquad (16)$$

$$\mathbf{G} = (G_k), \qquad k = 1, \ldots, N \qquad (17)$$

In the calculation of $\mathbf{F}$ in Eq. (16), flow depth was taken implicitly by weighing the consecutive flow depths in time

$$\mathbf{h}_{t*} = \alpha \mathbf{h}_{t-1} + (1-\alpha)\mathbf{h}_t \tag{18}$$

where

α – implicit weight coefficient

The solution to $\mathbf{h}_t$ was derived using the Newton-Rhapson method

$$\mathbf{G'}(\mathbf{h}_{t*})\,\Delta\mathbf{h}_{t*} = -\mathbf{G}(\mathbf{h}_{t*}) \tag{19}$$

$$\mathbf{h}_t = \mathbf{h}_t + \Delta\mathbf{h}_{t*} \tag{20}$$

where

$\mathbf{G'}(\mathbf{h}_{t*}) = (\partial G_{k,t*}/\partial h_{j,t*})_{k,j=1}^{N}$ = Jacobian Matrix

$\Delta\mathbf{h}_{t*} \equiv$ change of $\mathbf{h}_t$ between consecutive iterations

The Jacobian matrix was formed numerically by deviating the flow depth vector and subsequently, Eq. (19) was solved using the Thomas algorithm (Remson *et al.* 1971).

The parameters of the described models were estimated using the simplex procedure, minimizing the sum of the residual squared errors between the calculated and measured values (O'Neill 1971).

Assessment of the Prediction of the Runoff Models

The prediction of the models was assessed using a fitness coefficient which implied the efficiency of the model (Nash and Sutcliffe 1970)

$$R = \frac{\displaystyle\sum_{j=1}^{n_{max}}(x_j-\bar{x})^2 - \sum_{j=1}^{n_{max}}(x_j-\hat{x}_j)^2}{\displaystyle\sum_{j=1}^{n_{max}}(x_j-\bar{x})^2} \tag{21}$$

where

x_j – measured value
$\bar{x}$ – mean of the measured values
$\hat{x}_j$ – calculated value
n_{max} – number of the measurements

The highest fitness coefficient value was 1.

214

Results

Surface runoff was predicted first by using the transfer function model between measured rainfall and runoff Eq. (1). The model parameters were estimated separately with the simplex method for each runoff event. In the next case, the transfer function model for rainfall excess was used. The rainfall excess was evaluated by subtracting infiltrated water from the measured rainfall. The infiltration capacity Eq. (2) was reset to a large value after a six-hour dry period by setting the cumulative infiltration in Eq. (2) to a value close to zero. The six-hour dry period was selected after using different trial values. The evaluated rainfall excess was used as an input to the transfer function model Eqs. (3)-(4). In both empirical models, negative predictions were set to zero in the model runs.

In the physical models, the shape of the field sections was assumed to be a square subdivided into 10 node areas. Moreover, in the model runs, the 15-minute time interval of the measurements was divided by 8, yielding a time step of 1.875 minutes. As before, the infiltration capacity was reset to a large value after six hours of no rain and the negative predicted values were set to zero. The sheet flow model was formulated using Eqs. (9) and (12) and solved using the Euler and Newton-Rhapson methods as described in the previous section. The implicit weight coefficient, α, (was set to value 0.55 in the Newton-Rhapson method. Correspondingly, the rill flow model was formulated using Eqs. (11) and (12) and solved using the described methods. The dimensions of a rill were fixed in the following way. The cross section of a rill was assumed to be rectangular and the length equal to a side of the section. The width of the rill b_n was 0 at the upstream end and 10 cm at the downstream end of the section. The rill width values of the node areas between the ends were interpolated (see Fig. 7).

In the iterative simplex estimation, the parameters of the models were allowed to vary in wide ranges, which in the case of the physical models, were based on measurement or literature, and in the case of the empirical models, were chosen arbitrarily. The given ranges are shown in Table 2, and the results of the estimations are summarized in Table 3, which presents the sums of squared errors and the measured and

Table 2 – Parameter constraints in the estimation

Parameter	Range
a_1-a_3	(0.0, 1.0)
b_1-b_3	(0.0, 1.0)
K_a (mm/15 min)	(0.0, 300)
K_b (mm^2/15 min)	(0.0, 10)
n	(0.050, 5.0)
S (m/m)	(0.030, 0.070)
m (1/m)	(0.0, 10)

215

calculated cumulative surface runoff values. Fig. 8 gives the fitness coefficients of the calculated runoff events.

Finally, three estimated parameter combinations (those of June 22-23 and August 22-25 in Section 1, and October 11-14 in Section 2) were selected for testing of the models. The parameter combinations represented early summer, late summer, and autumn surface runoff characteristics. Using the fixed parameters, seven other runoff events were simulated; Figs. 9-11 summarize the fitness coefficients of the simulations.

Table 3 – Sums of squared errors and measured and calculated cumulative runoff values (mm) in parameter estimation of the models

	Jun 22-23, sec 1	Jul 24-25, sec 2	Aug 10-14, sec 1	Aug 17-21, sec 1	Aug 22-25, sec 1	Aug 23-25, sec 2	Oct 11-14, sec 1	Oct 11-14, sec 2
Meas sum	0.13	0.22	0.79	1.3	5.0	0.93	19	23
Transfer function model for overall rainfall								
Sqr err	0.0012	0.0015	0.0026	0.0036	0.12	0.019	3.9	1.9
Cal sum	0.15	0.25	0.53	1.3	5.0	1.2	26	27
Transfer function model for rainfall excess								
Sqr err	0.00048	0.00064	0.0023	0.0034	0.12	0.018	1.1	0.46
Cal sum	0.14	0.16	0.48	1.2	4.2	1.0	18	21
Sheet flow model solved by Euler								
Sqr err	0.0012	0.0026	0.0045	0.0049	0.13	0.013	3.7	1.1
Cal sum	0.89	0.10	0.27	0.60	4.5	1.1	11	17
Sheet flow model solved by Newton Rhapson								
Sqr err	0.00090	0.0024	0.0043	0.0050	0.16	0.015	2.0	0.63
Cal sum	0.057	0.12	0.30	0.48	4.1	0.61	14	18
Rill flow model solved by Euler								
Sqr err	0.00037	0.0017	0.0040	0.0045	0.12	0.016	3.7	1.3
Cal sum	0.083	0.12	0.37	0.64	4.5	0.64	14	19
Rill flow model solved by Newton Rhapson								
Sqr err	0.00025	0.0017	0.0040	0.0045	0.12	0.015	3.1	1.2
Cal sum	0.10	0.12	0.38	0.63	3.8	1.0	19	19

	Transfer function model for measured rainfall	Transfer function model for rainfall excess	Sheet flow model solved by Euler's method	Sheet flow model solved by Newton-Rhapson method	Rill flow model solved by Euler's method	Rill flow model solved by Newton-Rhapson method
a) Jun 22-23, Sec 1	0.57	0.84	0.58	0.69	0.87	0.91
b) Jul 24-25, Sec 2	0.71	0.88	0.51	0.55	0.67	0.68
c) Aug 10-14, Sec 1	0.50	0.57	0.15	0.19	0.23	0.23
d) Aug 17-21, Sec 1	0.33	0.36	0.08	0.07	0.15	0.15
e) Aug 22-25, Sec 1	0.63	0.64	0.62	0.51	0.65	0.64
f) Aug 23-25, Sec 2	0.45	0.47	0.61	0.56	0.53	0.56
g) Oct 11-14, Sec 1	0.69	0.91	0.71	0.84	0.71	0.76
h) Oct 11-14, Sec 2	0.84	0.96	0.91	0.95	0.89	0.91
Average	0.59	0.70	0.52	0.54	0.59	0.61

Fig. 8. Fitness coefficients of calculated runoff events using individual estimated parameters.

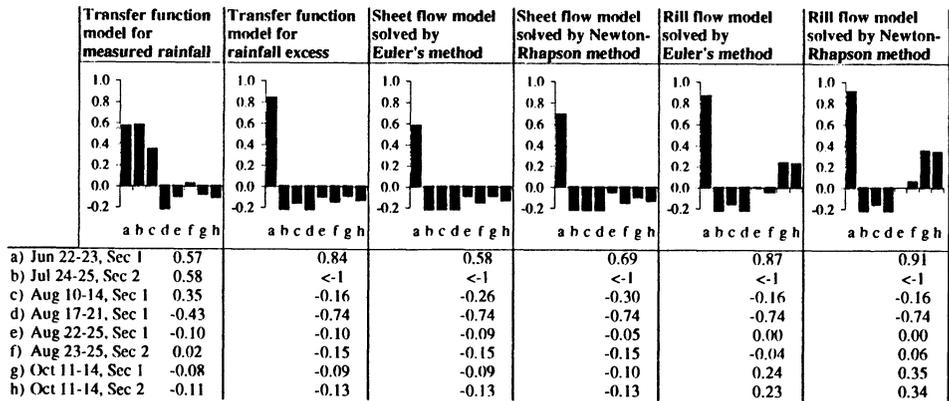|	Transfer function model for measured rainfall	Transfer function model for rainfall excess	Sheet flow model solved by Euler's method	Sheet flow model solved by Newton-Rhapson method	Rill flow model solved by Euler's method	Rill flow model solved by Newton-Rhapson method
a) Jun 22-23, Sec 1	0.57	0.84	0.58	0.69	0.87	0.91
b) Jul 24-25, Sec 2	0.58	<-1	<-1	<-1	<-1	<-1
c) Aug 10-14, Sec 1	0.35	-0.16	-0.26	-0.30	-0.16	-0.16
d) Aug 17-21, Sec 1	-0.43	-0.74	-0.74	-0.74	-0.74	-0.74
e) Aug 22-25, Sec 1	-0.10	-0.10	-0.09	-0.05	0.00	0.00
f) Aug 23-25, Sec 2	0.02	-0.15	-0.15	-0.15	-0.04	0.06
g) Oct 11-14, Sec 1	-0.08	-0.09	-0.09	-0.10	0.24	0.35
h) Oct 11-14, Sec 2	-0.11	-0.13	-0.13	-0.13	0.23	0.34

Fig. 9. Fitness coefficients of simulated runoff events using fixed parameters of June 22-23 event in Section 1.

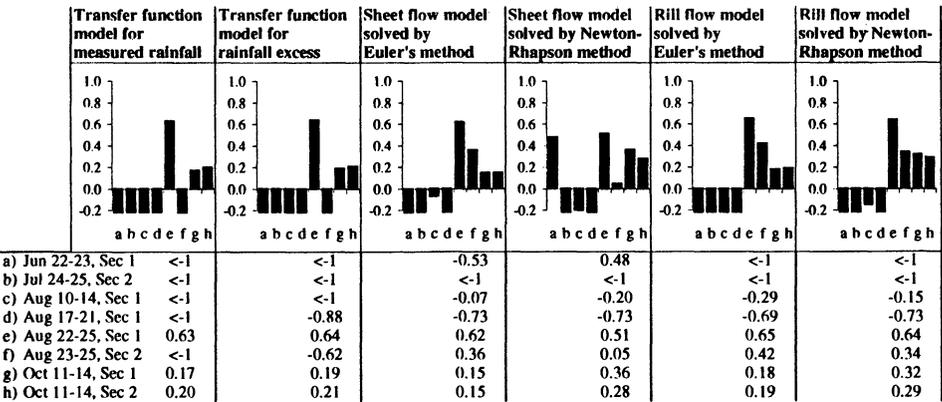|	Transfer function model for measured rainfall	Transfer function model for rainfall excess	Sheet flow model solved by Euler's method	Sheet flow model solved by Newton-Rhapson method	Rill flow model solved by Euler's method	Rill flow model solved by Newton-Rhapson method
a) Jun 22-23, Sec 1	<-1	<-1	-0.53	0.48	<-1	<-1
b) Jul 24-25, Sec 2	<-1	<-1	<-1	<-1	<-1	<-1
c) Aug 10-14, Sec 1	<-1	<-1	-0.07	-0.20	-0.29	-0.15
d) Aug 17-21, Sec 1	<-1	-0.88	-0.73	-0.73	-0.69	-0.73
e) Aug 22-25, Sec 1	0.63	0.64	0.62	0.51	0.65	0.64
f) Aug 23-25, Sec 2	<-1	-0.62	0.36	0.05	0.42	0.34
g) Oct 11-14, Sec 1	0.17	0.19	0.15	0.36	0.18	0.32
h) Oct 11-14, Sec 2	0.20	0.21	0.15	0.28	0.19	0.29

Fig. 10. Fitness coefficients of simulated runoff events using the fixed parameters of August 22-25 event in Section 1.

217

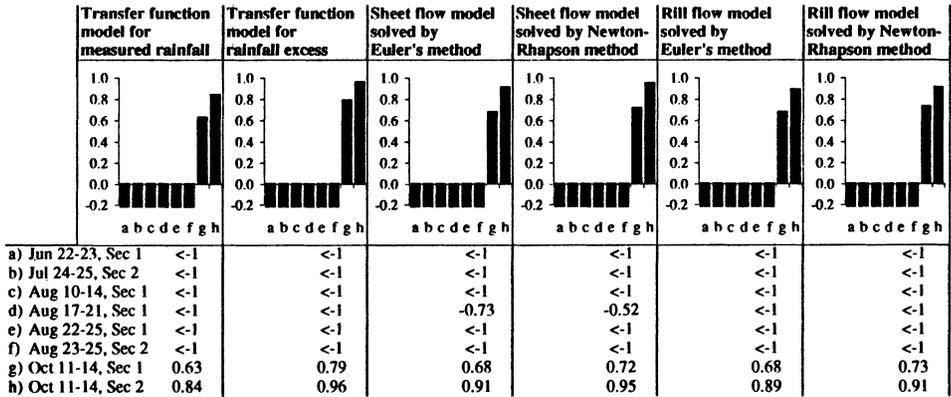|		Transfer function model for measured rainfall	Transfer function model for rainfall excess	Sheet flow model solved by Euler's method	Sheet flow model solved by Newton-Rhapson method	Rill flow model solved by Euler's method	Rill flow model solved by Newton-Rhapson method
a)	Jun 22-23, Sec 1	<-1	<-1	<-1	<-1	<-1	<-1
b)	Jul 24-25, Sec 2	<-1	<-1	<-1	<-1	<-1	<-1
c)	Aug 10-14, Sec 1	<-1	<-1	<-1	<-1	<-1	<-1
d)	Aug 17-21, Sec 1	<-1	<-1	-0.73	-0.52	<-1	<-1
e)	Aug 22-25, Sec 1	<-1	<-1	<-1	<-1	<-1	<-1
f)	Aug 23-25, Sec 2	<-1	<-1	<-1	<-1	<-1	<-1
g)	Oct 11-14, Sec 1	0.63	0.79	0.68	0.72	0.68	0.73
h)	Oct 11-14, Sec 2	0.84	0.96	0.91	0.95	0.89	0.91

Fig. 11. Fitness coefficients of the simulated runoff events using fixed parameters of October 11-14 event in Section 2.

Discussion

The runoff models were assessed on the basis of the fitness coefficients according to Eq. (21). Both the results of the estimation and the testing were considered.

In the parameter estimation, the transfer function model between surface runoff and rainfall excess performed best with respect to the fitness coefficients (Fig. 8). However, the model did not maintain the water balance, as the cumulative quantity of rainfall excess was larger than the cumulative surface runoff. The model was based on the presumption that rainfall excess would have been the runoff-generating component of the measured rainfall and that the transfer function model would have functioned as a hydrograph identifying the shape of the runoff curve (*e.g.*, Novotny and Shuhai 1989). The other empirical model, the transfer function model between runoff and measured rainfall, also performed relatively well in the estimation, but was deficient because it did not take into account changes in infiltration. The physical models did not function as well in parameter estimation as the transfer function model for rainfall excess. During early and late summer runoff events, the rill flow model solved by the Newton-Rhapson method performed best among the physical models, while the corresponding sheet flow model was better during autumn events. The Newton-Rhapson solution method was slightly better than the Euler solution. The sheet flow model solved by the Euler method showed the weakest overall performance in the estimation.

The estimated parameter values varied widely in the given ranges. During summer events, the time lag between rainfall and runoff peaks was small, resulting higher values for parameter b_1 compared to b_2 and b_3 in the transfer function models. Respectively, the parameters b_i had more uniform values during autumn events. The values of the parameters a_i indicated high autocorrelation in the runoff series. The infiltration parameters K_A and K_B did not show seasonal dependency in the transfer

218

function model. In the physical models, infiltration parameter K_B and roughness coefficient n gained smaller values during autumn events than summer events. During autumn, parameter K_B had even zero values. Other physical parameters did not show seasonal dependency, except parameter m in the rill flow model solved by Newton-Rhapson method. During autumn events, parameter m had higher values indicating that the number of rills in the section increased towards autumn.

The testing revealed model deficiencies under changing conditions. Using parameter combination of the runoff event in Section 1, June 22-23, only transfer-function model between measured rainfall and runoff was able to predict other early summer events (Fig. 9). Otherwise, the transfer function models had the weakest performance in the testing of the models, *e.g.*, the parameter combination of the runoff event in Section 1, August 22-25, was unable to predict the runoff event measured simultaneously in Section 2 (Fig. 10). Using the late summer parameter combination (Fig. 10), the rill flow models performed best of all the models, which was consistent with actual field conditions; surface runoff concentrated and formed rills in the sections. Both sheet and rill flow models had difficulties predicting small quantities of surface runoff under changing conditions, but the latter gained better fitness coefficients during late summer events. In the end, Fig. 11 showed that none of the models was capable to predict summer runoff events using autumn parameter combination.

The sources of errors in this analysis resulted from experimental arrangements, measurements, model structures, and estimation. The sides of the field sections were embanked, which did not correspond to the natural conditions under which surface runoff does not concentrate in only one outlet. The two sections studied were adjacent and runoff mixing between the sections was prevented by a small embankment. However, in times of intensive runoff mixing was difficult to prevent. During small events, some of the runoff bypassed the weir owing to the presence of small cracks and leaching.

Measurement errors included limits in the accuracy of the devices, voltage deviations, and inaccuracies in installation and calibration. The accuracy of the ultrasound sensor for water-level measurements was about $\pm 0.3\%$ of the distance between the sensor and the water level, which was about 40-60 cm. In addition, voltage deviations of the data logger accumulator increased the error. Precipitation was measured as an accumulation of water. Voltage deviations caused obvious errors in small rainfalls, which were excluded from the data as mentioned previously. Freezing during cold autumn nights caused additional erroneous pressures in the precipitation measurements which were most apparent in September. Finally, freezing temperatures broke the rain gauge in October. The measurement system was operated by the data logger and main computer programs. Changes to the programs resulting from addition of new devices frequently caused problems.

The tested models represented both empirical and physical approaches. Empirical transfer function models are usually used to predict the process one time step ahead.

219

Here, predicted (instead of the observed) values were used in the autoregressive part of the model because empirical models were required to predict the runoff based on one input only, the rainfall. However, the residual series were not analyzed, which the proper time series analysis would have required (Young 1984). The degrees of the polynomials were also limited to 3. Different degree compositions were examined and degree 3 was chosen to keep the number of the model parameters small.

The advantage of the physical models is that their parameters are theoretically measurable. In this case, restrictive assumptions were made which loosened the relevance of the model and its parameters from real conditions. Assumptions of uniform infiltration, roughness coefficient, and slope could not hold in the node areas. In the parameter estimation, prediction by the physical models was improved by letting the parameters, including slope, vary over wide ranges. In the comparison of the models, the predictions were assessed against runoff events of variable cumulative quantities. The early summer surface runoff peaks were small compared with the intensive late summer and autumn events; therefore, the importance of early summer events was overrated. The model testing was performed using event based parameter calibration. Figs. 9-11 showed that the models failed to predict runoff under changing conditions, which was due to deficient model structures with fixed parameters. The parameter estimation over continuous summer and autumn data would be preferred, but in this case, continuous simulation would require the use of time dependent model parameters. Using fixed parameters estimated over continuous data, the models would have predicted the highest autumn peaks only.

The summer and autumn runoff series showed that equal rainfall peaks produced various amounts of surface runoff at different times. Saturation of the soil toward autumn had a significant influence on infiltration, while the six-hour dry periods did not have the assumed effect on infiltration capacity. A more proper model for the infiltration capacity would have been a two dimensional soil-water model, which would have simulated the water flow in saturated-unsaturated soil and which would have given the overland flow on the exfiltration part of the section (Troendle 1985).

Parameter estimation of the models was done using the simplex procedure. Estimation and convergence were rapid with the transfer function models. In the case of the physical models and especially the Newton-Rhapson method, parameter estimation was time-consuming and convergence depended considerably on the initial parameter values.

Conclusions

The rainfall runoff data of the experimental field indicated that the proportional quantity of runoff depends considerably on the antecedent conditions in soil moisture and groundwater level. Even the largest summer storms generated hardly any runoff when the soil was dry and well-cracked. After the groundwater level reached the topsoil layers, the amount of surface runoff increased.

220

In parameter estimation, the transfer function model between rainfall excess and surface runoff performed best with respect to the fitness coefficients. The rill flow model solved by the Newton-Rhapson method was the best-performing physical model. Testing of the models using fixed parameter combinations showed that the models were unable to predict the runoff under changing conditions. An event based estimation was not applicable in verifying the models to different conditions. A continuous simulation of surface runoff would be preferred, which however, would require the use of time dependent parameters. During summer, the cracks are a characteristic feature in clayey soils in Finland, which phenomenon was not able to be modeled using a fixed parameter model for infiltration capacity. A more proper model for the infiltration would be a two dimensional soil-water model simulating the water flow in saturated-unsaturated soil. The presented sheet and rill flow models would be used to route the overland flow on the exfiltration area of the sections.

This study dealt with warm-season surface runoff on an agricultural field in southern Finland. Much of the runoff takes place when snow melts during spring. Evaluation of runoff models for all seasons would require measurements and description of the snowmelt processes.

Acknowledgements

References

Conte, S. D., and de Boor, C. (1981) *Elementary Numerical Analysis, An Algorithmic Approach*, McGraw-Hill International Editions, Singapore, 432 pp.

Evans, R. O., Gilliam, J. W., and Skaggs, R. W. (1989) Effects of agricultural water table management on drainage water quality, Report No. 237, Water Resources Research Institute of the University of North Carolina, Raleigh, NC, 87 pp.

Jakeman, A. J., Littlewood, I. G., and Whitehead, P. G. (1990) Computation of the instantaneous unit hydrograph and identifiable component flows with application to two small upland catchments, *J. Hydrol., Vol. 117*, pp. 275-300.

Kauppi, L. (1982) Testing the applicability of the CREAMS model to estimation of agricultural nutrient losses in Finland, Publications of the Water Research Institute, National Board of Waters, Finland, 49, pp. 30-39.

Laikari, E., and Karvonen, T. (Ed.) (1992) Säätösalaojitus – Koekenttien perustaminen (with English summary: Controlled drainage and subirrigation as a method for reducing nutrient loading from agricultural fields) Finnish Field Drainage Research Society, Report No. 16, 64 pp.

221

Li, R.-M., Simons, D.B., and Stevens, M.A. (1975) Nonlinear kinematic wave approximation for water routing, *Water Resour. Res., Vol. 11* (2), pp. 245-252.

Mustonen, S. (1963) Kesäsateiden aiheuttamasta valunnasta (with English abstract: On the runoff due to summertime rainfall) Soil and Hydrotechnical Research Office, Report 3, 90 pp.

Nash, J. E., and Sutcliffe, J. V. (1970) River flow forecasting through conceptual models, Part I – A discussion of principles, *J. Hydrol., Vol. 10*, pp. 282-290.

Novotny, V., and Shuhai, Z. (1989) Rainfall-runoff transfer function by ARMA modeling, *J. Hydr. Engrg., ASCE Vol. 115 (10)*, pp. 1386-1400.

O'Neill, R. (1971) Algorithm AS 47, Function minimization using a simplex procedure, *Applied Statistics, Vol. 20*, pp. 338-345.

Parlange, J.-Y., Rose, C. W., and Sander, G. (1981) Kinematic flow approximation of runoff on a plane: An exact analytical solution; *J. Hydrol., Vol. 52*, pp. 171-176.

Pearson, C. P. (1989) One-dimensional flow over a plane: Criteria for kinematic wave modelling, *J. Hydrol., Vol. 111*, pp. 39-48.

Rekolainen, S., and Posch, M. (1993) Adapting the CREAMS model for Finnish conditions, *Nordic Hydrology, Vol. 24 (5)*, pp. 309-322.

Remson, I., Hornberger, G. M. and Molz, F. J. (1971) *Numerical methods in subsurface hydrology*, New York, Wiley Interscience, 389 pp.

Seuna, P. (1983) Small basins – a tool in scientific and operational hydrology, Publications of the Water Research Institute, National Board of Waters, Finland, 51, 61 pp.

Skaggs, R. (1980) A water management model for shallow water table soils, Report No. 134. Water Resources Research Institute of the University of North Carolina, Raleigh, NC, 53 pp.

Troendle, C. A. (1985) Variable source area models. In: *Hydrological Forecasting* (Ed.) Anderson, M. G., and Burt, T .P., John Wiley and Sons Ltd, pp. 347-403.

Young, P. (1984) *Recursive Estimation and Time Series Analysis, An Introduction*, Springer-Verlag, Berlin, Germany, 300 pp.

Wooding, R. A. (1965) A hydraulic model for the catchment-stream problem I. Kinematic-wave theory, *J. Hydrol., Vol. 3*, pp. 254-267.

Address:
Helsinki University of Technology,
Laboratory of Water Resources Engineering,
Konemiehentie 2,
FIN-02150 Espoo,
Finland